Synthesizing Ag/PDA/PES Antibacterial Membrane for Natural Organic Molecules Removal

Kok Poh Wai[1], *Chai Hoon* Koo[1*], *Yean Ling* Pang[1], *Woon Chan* Chong[1] and *Woei Jye* Lau[2]

[1]Lee Kong Chian Faculty of Engineering and Science, Universiti Tunku Abdul Rahman, Jalan Sungai Long, 43000 Kajang, Selangor, Malaysia.
[2]Advanced Membrane Technology Research Centre (AMTEC), Universiti Teknologi Malaysia, 81310 Skudai, Johor, Malaysia.

Abstract. Silver nanoparticles (NP) was successfully immobilized on polydopamine (PDA) supported polyethersulfone (PES) membrane via a redox reaction. Polyvinylpyrrolidone (PVP) was added into membrane dope solution as a pore-forming agent. Four pieces of membranes (M1, M2, M3 and M4) were fabricated with different active layer coatings to compare their morphological and performance properties. The differences between each sample were highlighted as follow: M1 (pristine PES), M2 (PES+PVP), M3 (PDA/PES+PVP) and M4 (Ag/PDA/PES+PVP). All membranes were characterized using scanning electron microscopy, energy dispersive X-ray spectroscopy, Fourier-transform infrared spectroscopy, X-ray diffraction and contact angle analysis. The membrane performance was examined using pure water permeability (PWP) test, antibacterial test and humic acid (HA) rejection test. Pristine M1 membrane showed that PWP of 27.16 LMH/bar and HA rejection of 84 %. In this study, it was found that the addition of PVP as a pore agent into the membrane M2 increased water flux but slightly deteriorated HA rejection. Coating of PDA on M3 and immobilizing silver NP on M4 membrane surface have improved HA rejection but compromised PWP. The results showed that membrane M4 carried excellent antibacterial property and highest HA rejection among all fabricated membranes.

1 Introduction

Polyethersulfone (PES) has been a promising material for synthesizing polymeric membrane and used in various industries, such as protein separation, pharmaceuticals product separation, wastewater treatment, gas separation, beverage concentration and particulate removal [1]. In facts, PES possesses many desirable properties over other candidates, including high chemical resistance, wide pH tolerance, low cost, resist chlorine attack, good miscibility with additives and solvents. However, membrane surface properties have a great influence on its ability to resist fouling, which includes surface roughness, surface charges and hydrophilicity. Critically, Rahimpour et al. reported that the

* Corresponding author: kooch@utar.edu.my

hydrophobic characteristic of PES caused serious fouling in membrane process due to deposition of molecules on membrane surface and pores [2]. Hence, there is a necessity to tailor the membrane surface properties to yield outstanding anti-biofouling performance and longer service lifespan.

The existence of natural organic molecules (NOM) in surface water sources caused undesired colour and taste in water body. Besides, NOM forms complexes with heavy metals, pesticides and chlorine. Among others, humic substances constitute as a major fraction in surface water NOM, typically ranged from 50 to 80 %. Hamid et al. mentioned that humic substances can be categorised into humin, fulvic acid and humic acid (HA) according to their solubility at different pH [3]. Carboxylic, phenolic alcohols and methoxyl carbonyls in HA molecules have the potential to react with other organic compounds, which then produces carcinogenic chlorinated by-products such as trihalomethane and haloacetic acid. As the major constituent in NOM, HA is therefore widely adopted as a model organic pollutants in water research and become the benchmark for NOM removal in membrane-related studies [3].

Biofouling, the critical problem faced by membrane technology, can be mitigated by enhancing surface hydrophilicity. The membrane hydrophilicity can be improved by surface modification [4]. Polydopamine (PDA), a bio-inspired polymer, is able to reduce fouling caused by oil/water emulsion [5]. In recent years, adopting PDA coating on membrane surface as to improve membrane wettability becomes a new direction in membrane research [6, 7]. It was reported that PDA showed a good stability on membrane surface due to strong covalent and non-covalent interactions with the substrate. Polymerization of dopamine also introduces new functional groups such as catechol and amine which are hydrophilic. PDA could serve as a 'bioglue', where the catechol, quinone and amine groups of PDA could allow further reactions with functional molecules.

Numerous studies showed that incorporating silver NP into membrane matrix or onto membrane surface could promote antibacterial properties, hence reduce the likelihood of biofouling. Xiu and coworkers reported that silver act as antibacterial agent when it was brought in contact with bacteria or released as ion [8]. Interaction between silver and thiol groups (S-H) in cysteine will destabilize protein and destroys bacterial cell membrane [9-11]. Hence, direct interaction between silver and bacterial cell lead to formation of hole and pits on cellular surface, which then induces leakage of cytoplasmic material and loss of morphological integrity [12]. On top of that, dissolution of positively-charged silver ion from silver NP is responsible for the electrostatic attraction towards negatively charged bacteria cell membrane [13], for which it would disrupt electron transport chain and causes DNA dimerization. Hence, silver ions uptake by bacteria cell not only causing the inhibition of DNA replication [14] but also contributes to apoptosis [15].

In facts, many researchers are developing membrane with loaded silver NP as to mitigate biofouling problems caused by microorganism [15]. For example, Wu et al. claimed that PDA could be used as both a polymer linker and reductant to achieve silver coating [29]. Dopamine has metal ion chelating ability and redox activity [16] in which it can readily reduce the adsorbed silver ion to form silver NP in one step reaction [17]. The bifunctional performance of PDA serves as a simple and effective route for in situ silver reduction, thus becomes a practical approach for surface immobilization of silver NP [18].

2 Experimental

2.1 Materials

Polyethersulfone (PES, granule, MW = 35,000 g/mol, Solvay, UK) was chosen as the base polymeric material while N-methylpyrrolidinone (NMP, ≥ 99.5 %, Merck, Germany) was

selected as solvent to dissolve PES polymer. Polyvinylpyrrolidone (PVP, powder, MW = 29,000 g/mol, Sigma-Aldrich, Germany) was used as pore-forming agent. Dopamine hydrochloride (powder, Sigma-Aldrich, Germany) and hydrochloride buffer solution (Tris-HCl, 1M, Sigma-Aldrich, Germany) were used to synthesize a layer of PDA on PES membrane. Immobilization of silver NP was done by in situ silver ions reduction on PDA layer using silver nitrate solution (2.5 w/v % $AgNO_3$ in H_2O, Sigma-Aldrich, Switzerland). Humic acid (powder, 4710 g/mol, Sigma-Aldrich, Switzerland) was used as the solution model for membrane solute rejection studies while sodium bicarbonate (≥ 99 %, Chemsoln, Malaysia) was added to improve humic acid solubility in water. The distilled water used in this study was obtained from a laboratory distillation unit (Favorit W4L Water Stills, Malaysia). All reagents were of analytical grade and used as received.

2.2 Membrane fabrication

Table 1 summarises the dope compositions and surface modifications of membranes. PES and PVP were dried in oven at 60 °C for 24 hours to remove moisture. For membrane M1 (control), 30 g of dope solution was prepared by dissolving 25 wt% of PES in 75 wt% of NMP under continuous stirring at 50 °C to ensure its homogeneity. For membrane M2, M3 and M4, 25 wt% of PES and 6 wt% of PVP (pore forming agent) were dissolved in 20.7 g of NMP under similar condition. The homogenous dope solution was left cooled for 30 minutes before it was poured on a glass plate. Adjustable film applicator (Braive Instrument, Germany) was used to cast the membrane at 150 µm. The wet polymeric film was immediately immersed into distilled water bath at room temperature for phase inversion. A flat sheet membrane was formed and stored wet at room temperature prior to usage.

Table 1. Membrane composition and coating layer.

Sample	Dope	Coating
M1	25 % PES + 75 % NMP	-
M2	25 % PES + 6 % PVP + 69 % NMP	-
M3	25 % PES + 6 % PVP + 69 % NMP	PDA
M4	25 % PES + 6 % PVP + 69 % NMP	Ag/PDA

2.3 Membrane surface modification

Membrane M3 and M4 were fixed on a 10 cm x 15 cm acrylic frame with the active surface exposed to coating reagent. The dopamine solution (2 g/L) was prepared by dissolving 200 mg of dopamine hydrochloride in 100 mL Tris-HCl buffer solution (pH = 8.5, 0.05M). The solution was poured on the active surface of the membrane and left open to air for 4 hours. Dopamine will gradually oxidize and form a layer of PDA on the membrane active surface. The membranes were rinsed with distilled water several times and stored wet. For membrane M4, 50 mL of silver nitrate solution (1 g/L) was poured on its active surface (after PDA coating) and left for 2 hours. The membrane was then rinsed with distilled water several times and stored wet.

2.4 Membrane characterization

The cross-sectional morphologies of the membranes were studied using scanning electron microscopy (SEM, Hitachi S3400N, Japan). Prior to the analysis, the samples were dried

overnight in 60 °C oven, cracked in cryogenic liquid nitrogen and sputtered with gold (Quorum SC7620, UK). Energy dispersive X-ray spectroscopy (EDX) was used to identify the elements present in each membrane samples. The bonding of functional groups on the membrane surface was analyzed using Fourier-transform infrared spectroscopy (FTIR, Thermo Scientific Nicolet iS10, USA). The transmission spectra were recorded from 400 to 4000 cm^{-1} after baseline correction and the resolution was 4 cm^{-1}. The reduced silver NP formed on membrane M4 was characterized by X-ray diffractometer (XRD, Shimadzu 6000, Cu-Kα radiation) at 40 kV and 0.3 mA. The diffraction pattern on 2θ from 5° to 85° was collected at the scanning rate of 5° per minute. Membrane wettability was examined by sessile drop method using contact angle goniometer (KRÜSS GmbH, Germany). About 0.2 µL of distilled water was dropped on the active surface of the membrane and the contact angle was measured immediately. The measurement was repeated for four times at different locations and the values were averaged to obtain a mean.

2.5 Membrane performance study

2.5.1 Permeability, pore size, porosity, pore radius

Water permeability of synthesized membranes was evaluated by using a dead-end filtration cell (Sterlitech™ HP4750) with 14.6 cm^2 of active area. Membrane samples were cut into circular shape with 49 mm diameter, then pressurized under compaction of 10 bar for 30 minutes before pure water permeability (PWP) test was conducted. PWP was calculated using Eq. (1) [19],

$$PWP = \frac{Q}{A \times \Delta t \times \Delta p} \tag{1}$$

where Q represents permeate volume in L, A is the membrane area in m^2, Δt is the time taken to collect the permeate in hour and Δp represents the operational pressure in bar. Membrane porosity (ε) was calculated using Eq. (2) [19],

$$\varepsilon = \frac{(W_1 - W_2)/\rho_{water}}{(W_1 - W_2)/\rho_{water} + W_2/\rho_{membrane}} \times 100\% \tag{2}$$

where W_1 represents the weight of wet membrane. It was measured by using analytical balance after storing the membrane in distilled water overnight. W_2 is the weight of dry state membrane. It was measured after drying the same piece of membrane in 60 ºC oven for 24 hours. Both W_1 and W_2 are in unit kg. ρ_{water} and $\rho_{membrane}$ are the density of water and membrane in dry state, respectively. The pore radius (r_m) was calculated using Eq. (3) [4],

$$r_m = \sqrt{\frac{(2.9 - 1.75\,\varepsilon) \times 8\,\eta\, l\, Q}{\varepsilon \times A \times \Delta P}} \tag{3}$$

where l represents the thickness of the membrane in m, η stands for the viscosity of pure water in Pa.s whereas ΔP is the transmembrane pressure in Pa.

2.5.2 Humic acid rejection

Humic acid (HA) was chosen as the model NOM compound in the study. 10 ppm HA solution was fed into the dead-end filtration cell to conduct the solute rejection test. UV-visible spectrophotometer (PG Instrument, T60U) was adopted to measure the UV absorbance of the HA feed and permeate samples at 254 nm [3]. A calibration curve of absorbance against concentration of HA was drawn based on 2, 4, 6, 8 and 10 ppm of HA solution. By using the calibration curve, the absorbance value can be converted to instantaneous concentration of HA, where its rejection was subsequently calculated via Eq. (4) [4, 19]. C_p and C_f represent the concentration of HA in ppm for permeate and feed, respectively.

$$R_{HA}\% = \left(1 - \frac{C_p}{C_f}\right) \times 100\% \quad (4)$$

2.5.3 Antibacterial test

The antibacterial properties of the membranes were investigated via disk diffusion assay. 200 µL of inoculum contained *Escherichia coli* (*E. coli*) was dropped and spreaded on sterilized agar plate. Membrane samples were cut in circular-shaped with diameter of 1.5 cm, then placed on the agar plate with its active surface facing the nutrient agar. The agar plates were sealed with parafilm and incubated overnight at 37 °C. The diameter of bacterial inhibition zone, defined as zone around the disk where no bacteria growth was observed.

3 Results and discussion

3.1 SEM-EDX

The cross-sectional SEM images of synthesized membranes were shown in Fig. 1. The membranes are having finger-like structure at their top sublayer and microvoids at bottom sublayer. The instantaneous demixing of polymers and solvent during phase inversion gave rise to the formation of the membrane. From Fig. 1. (a), membrane M1 shows tightly packed finger-like structure at top sublayer. According to Chong et al., membrane fabricated without the addition of PVP as pore agent would show a short finger-like and spongy structure [20]. This was probably caused by the slower phase inversion rate owing to the hydrophobic nature of PES. With the addition of 6 wt% of PVP as pore agent, membrane M2, M3 and M4 displayed macrovoids at the bottom sublayer and loosely packed finger-like structure at top sublayer. As mentioned in Peydayesh's work, introducing PVP into dope solution will increase solution viscosity and reduce diffusion coefficient. Thermodynamic enhancement caused higher demixing rate between solvent and non-solvent, reduced kinetic hindrance [21] and yielded the final morphologies in Fig. 1. In addition, membrane M1 fabricated without PVP is having a denser structure as compared to M2, M3 and M4.

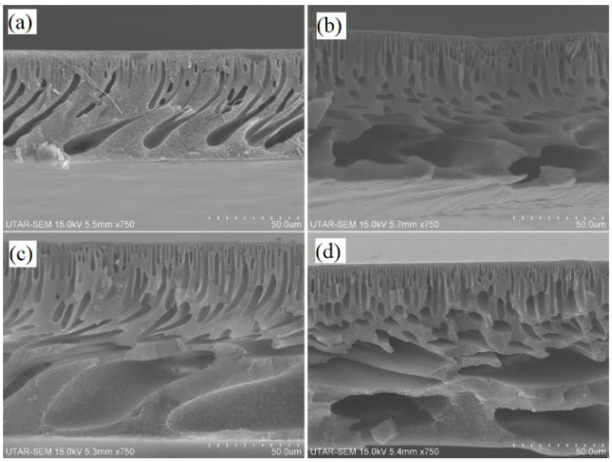

Fig. 1. Cross-sectional view of membranes (a) M1 (b) M2 (c) M3 (d) M4 at 750x magnification.

The EDX spectra were used to determine elemental composition of the fabricated membrane and being tabulated in Table 2. Membrane M1 and M2 show similar carbon, sulphur and oxygen content whereby the composition was in agreement with those reported by Zhang et al. [7]. No trace elements were found in M1 and M2, indicates that pristine PES membranes were produced. The existence of 2.49 at% of nitrogen was contributed by PDA coating in which Huang et al. have reported the same observation [22]. Upon silver nitrate treatment, 1.78 at% or 11.56 wt% of silver was found in EDX spectra of membrane M4. This confirms that silver nitrate has been successfully reduced to silver NP and immobilized on the PDA layer. The crystallinity of synthesized silver NP was studied thoroughly in XRD analysis.

Table 2. Atomic percentage of elements from EDX spectral.

Membrane	Atomic per cent (at%)				
	C	S	O	N	Ag
M1	72.12	17.50	10.38	-	-
M2	73.02	17.53	9.45	-	-
M3	72.31	10.14	15.06	2.49	-
M4	63.36	10.18	19.68	5.00	1.78

3.2 FTIR

Fig. 2. shows the FTIR spectra of fabricated membranes. All membranes show similar FTIR spectra as they are having the same PES substrate. The C-H stretching peak of benzene ring contributes to a broad band at 3080 cm^{-1} [23]. The existence of C-O-C stretching peak was confirmed at 1240 cm^{-1} [24] whereas aromatic skeletal vibration was observed at 1420 cm^{-1} [25]. The aromatic C-C stretching was captured at 1580 cm^{-1} while S=O stretching peak caused by sulfone group were recorded at 1130 and 1170 cm^{-1} [24]. For membrane M3 and M4, PDA shows absorption peaks at 1610 cm^{-1} due to N-H bending vibration and aromatic ring stretching, as well as 3400 cm^{-1} owing to the vibration of catechol OH groups and N-H groups [22]. However, these peaks for PDA is not significant in this study due to the nature of PDA being a thin coating and overlapping peaks [22, 24]. Absorption peak at 1660 cm^{-1} for membrane M2, M3 and M4 were caused by PVP

molecules that attached on PDA layer via hydrogen bonding between C=O of PVP and N-H of PDA [22], which is not shown in M1 spectrum. On the other hand, FTIR spectra for silver is not visible because the amount of silver present in the membrane is far below the detection limit [26]. In addition, FTIR is not suitable for the detection of inorganic compound.

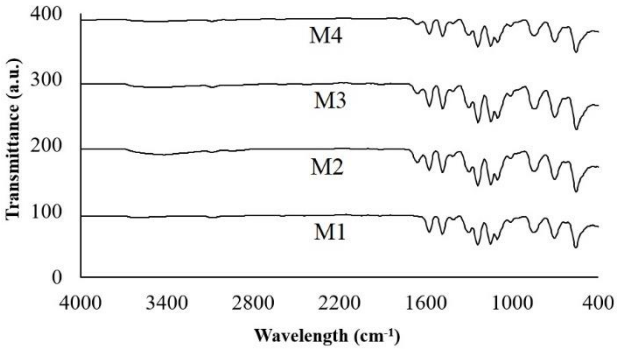

Fig. 2. FTIR spectra for membrane M1, M2, M3 and M4

3.3 XRD

XRD was used for determining the crystalline structure of the immobilized silver NP on PDA/PES membrane. Membrane M1, M2 and M3 were made up of polymers, thus XRD cannot be used for characterization of the amorphous samples. Fig. 3. shows the diffraction pattern of M4 membrane. A broad peak that observed at 20° in the 2θ range corresponded to an amorphous structure [15]. The sharp peaks at 37.8°, 43.8°, 64.2°, 77.2° and 81.5° were representing the (1 1 1), (2 0 0), (2 2 0), (3 1 1) and (2 2 2) planes of the face-centered cubic lattice of silver NP (JCPDS 04–0783). The existence of silver NP was confirmed while its bactericidal effect was further justified in the antibacterial test.

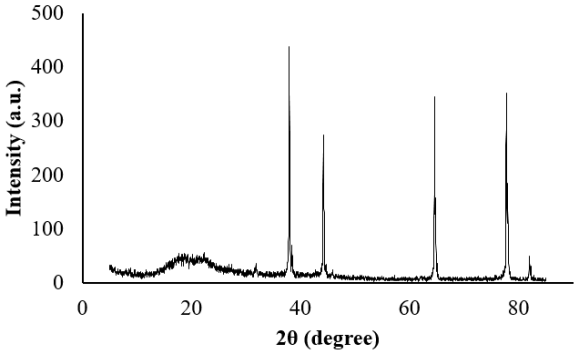

Fig. 3. XRD diffraction pattern for membrane M4.

3.4 Contact angle

Table 3 depicts the contact angle values for fabricated membranes. Considering that PES is a hydrophobic material [2], the contact angle of pristine PES membrane was found to be 71.68°. By adding 6 wt% of PVP into casting solution, the contact angle for M2 increased to approximately 75°. The membrane surface becomes more hydrophobic despite the formation of smaller pores and higher porosity in the membrane matrix. Similar observation

was reported in Vatsha et al., who found contact angle of membrane increased as PVP loading is greater than 4 wt% [27]. The PDA coating on M3 membrane successfully improved surface hydrophilicity and reduced contact angle by 2.84°. Similar findings were reported in the literature, owing to the hydrophilic nature of catechol, quinone and amine groups in PDA [5, 22]. The authors also claimed that hydrophilic PDA has the tendency to improve membrane wettability and repels hydrophobic foulants such as proteins and emulsified oil droplets. Immobilization of hydrophilic silver NP [24] on membrane M4 further reduced the contact angle to 68.27°, similar to those reported in Huang et al. [22]. Hence, it can be assured that coating of hydrophilic dopamine and immobilization of hydrophilic silver NP could improve membrane wettability, justified by the lower contact angle values.

Table 3. Contact angle of fabricated membranes.

Membrane	Contact Angle
M1	71.68° ± 1.97°
M2	75.07° ± 2.73°
M3	72.23° ± 0.57°
M4	68.27° ± 1.26°

3.5. Permeability, pore size, porosity, pore radius

From Table 4, membrane M2, M3 and M4 with 6 wt% PVP shows higher porosity than pristine membrane M1. The PWP of membrane M2 increased more than threefold with the addition of 6 wt% PVP as pore agent, as compared to the pristine M1 membrane. Enlargement of pore size and porosity was believed to be a major factor [4]. In contrast, the coating of PDA caused pore blockage, reduced mean pore radius as well as PWP, similar to those reported in the literature [7]. Immobilization of silver NP on membrane M4 further reduced the PWP to 10.66 LMH/bar as the silver NP aggregates covered up surface and reduced mean pore size [22]. Besides, increasing silver content in membrane shall decrease water flux due to barrier effect promoted by the presence of silver NP in the membrane surface and pores [28].

Table 4. PWP, porosity and mean pore radius of fabricated membranes.

Membrane	PWP (LMH/bar)	Porosity (%)	Mean pore radius (nm)
M1	27.16	42.02	15.34
M2	89.86	48.16	26.14
M3	25.83	48.49	15.42
M4	10.66	49.21	9.35

It is worth to mention that all the fabricated membrane are having their pore radii in the ultrafiltration range, which is between 1 and 100 nm [1, 22]. Introducing 6 wt% of PVP in the membrane M2 caused a higher membrane porosity and larger pore size. For membrane M3, dopamine solution penetrated into membrane pores, oxidized and polymerized in the matrix [22]. PDA nanoaggregates were formed on the surface and concentrated in the top layer cross-section, which is believed to yield smaller pore size. The silver nitrate treatment induced silver NP formation at the PDA surface, blocks pores and further reduces pore size. Besides, silver ions trigger oxidation of residual catechol groups on PDA, where the self-

crosslinking reaction between PDA oligomers was initiated and caused the formation of membrane with smaller pore size [7].

3.6 Humic acid rejection

From Table 5, pristine PES M1 membrane shows 84.2 % of HA rejection. Introducing 6 wt% of PVP into membrane M2 successfully improved permeation flux, however, it was accompanied by a lower HA rejection possibly due to the enlargement of pore size by 50 %. With a layer of PDA coating, HA rejection of membrane M3 was improved to 92.4 %. Zhang et al. claimed that PDA deposition caused pore blockage and yielded higher rejection [7]. After silver nitrate treatment, the formation of silver NP aggregates on membrane M4 further reduced the pore size and recorded the highest HA rejection at 95 %.

Table 5. HA rejections of fabrication membranes.

Membrane	HA Rejection %
M1	84.2
M2	78.1
M3	92.4
M4	95.1

3.7 Antibacterial test (ZOI)

The antibacterial activities of the fabricated membrane were first investigated by disk diffusion method. Fig. 4. shows the results for zone of inhibition test. Numerous *E. coli* colonies were found on the agar plates after 24 hours incubation at 37 °C. No bacteria inhibition against *E. coli* was observed in membrane M1, M2 and M3. In contrast, a clear inhibition zone was formed around membrane M4, indicates that Ag/PDA/PES membrane possesses significant bactericidal effect. It was believed that the presence of silver NP contributes to antibacterial properties, similar to those reported in the literature [8-13].

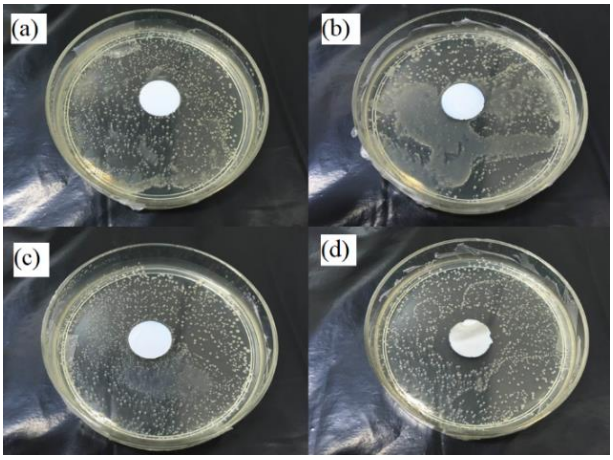

Fig. 4. ZOI of fabricated membrane (a) M1 (b) M2 (c) M3 (d) M4.

4 Conclusion

In this study, hydrophilic PDA layer was synthesized on pristine PES membrane via monomers oxidation. Then, silver NP was immobilized on PDA supported PES membrane by silver nitrate reduction method. Four membranes were produced in this study, namely M1 (pristine PES), M2 (PES+PVP), M3 (PDA/PES+PVP) and M4 (Ag/PDA/PES+PVP). Comparing pristine membrane M1, the addition of PVP into M2 dope solution induced formation of larger pores and higher porosity, which then increased PWP by threefold. Coating of hydrophilic PDA on M3 membrane increased membrane wettability and yielded higher HA rejection. Immobilizing silver NP on the PDA layer in M4 membrane further enhanced HA rejection but compromised PWP. The XRD and EDX analysis confirmed the existence of silver NP that successfully immobilized on the membrane surface. The bactericidal effect of membrane M4 was demonstrated in the zone of inhibition study. In conclusion, the Ag/PDA/PES membrane (M4) displayed the optimum HA rejection along with excellent antibacterial performance. The enhanced hydrophilicity of M4 shows better anti-biofouling characteristic as compared to other fabricated membranes.

The authors wish to express their gratitude to Universiti Tunku Abdul Rahman (UTAR) for providing financial support (Project no.: IPSR/RMC/UTARRF/2016-C1/K2).

References

1. M. Omidvar, M. Soltanieh, S.M. Mousavi, E. Saljoughi, A. Moarefian, H. Saffaran, J Environ Health Sci Eng. **13**, 42 (2015)
2. A. Rahimpour, S.S. Madaeni, J Memb Sci. **360**, 371-379 (2010)
3. N.A.A. Hamid, A.F. Ismail, T. Matsuura, A.W. Zularisam, W.J. Lau, E. Yuliwati, M.S. Abdullah, Desalination. **273**, 85-92 (2011)
4. H. Basri, A.F. Ismail, M. Aziz, Desalination. **273**, 72-80 (2011)
5. B.D. McCloskey, H.B. Park, H. Ju, B.W. Rowe, D.J. Miller, B.J. Chun, K. Kin, B.D. Freeman, Polymer. **51**, 3472-3485 (2010)
6. Y. Li, Y. Su, X. Zhao, X. He, R. Zhang, J. Zhao, X. Fan, Z. Jiang, ACS Appl Mater Interfaces. **6**, 5548-57 (2014)
7. R. Zhang, Y. Su, L. Zhou, T. Zhou, X. Zhao, Y. Li, Y. Liu, Z. Jiang, RSC Adv. **6**, 32863-32873 (2016)
8. Z.M. Xiu, Q.B. Zhang, H.L. Puppala, V.L. Colvin, P.J. Alvarez, Nano Lett. **12**, 4271-5 (2012)
9. K. Zodrow, L. Brunet, S. Mahendra, D. Li, A. Zhang, Q. Li, P.J. Alvarez, Water Res. **43**, 715-23 (2009)
10. M.S. Mauter, Y. Wang, K.C. Okemgbo, C.O. Osuji, E.P. Giannelis, M. Elimelech, ACS Appl Mater Interfaces. **3**, 2861-8 (2011)
11. Y. Liu, E. Rosenfield, M. Hu, B. Mi, Water Res. **47**, 2949-2958 (2013)
12. W.R. Li, X.B. Xie, Q.S. Shi, H.Y. Zeng, Y.S. Ou-Yang, Y.B. Chen, Appl. Microbiol. Biotechnol. **85**, 1115-22 (2010)
13. J.S. Kim, E. Kuk, K.N. Yu, J.H. Kim, S.J. Park, H.J. Lee, S.H. Kim, Y.K. Park, Y.H. Park, C.Y. Hwang, Y.K. Kim, Y.S. Lee, D.H. Jeong, M.H. Cho, Nanomedicine. **3**, 95-101 (2007)
14. L. Guo, W. Yuan, Z. Lu, C.M. Li, Colloids Surf. A. **439**, 69-83 (2013)
15. P.F. Andrade, A.F. de Faria, S.R. Oliveira, M.A. Arruda, C. Goncalves Mdo, Water Res. **81**, 333-42 (2015)
16. K. Fan, A. Granville, Polymers. **8**, 81 (2016)

17. A. GhavamiNejad, L.E. Aguilar, R.B. Ambade, S.-H. Lee, C.H. Park, C.S. Kim, J. Colloid Interface Sci. **6**, 5-8 (2015)
18. J. Wang, Y. Wu, Z. Yang, H. Guo, B. Cao, C.Y. Tang, Sci Rep. **7**, 2334 (2017)
19. S. Mokhtari, A. Rahimpour, A.A. Shamsabadi, S. Habibzadeh, M. Soroush, Appl. Surf. Sci. **393**, 93-102 (2017)
20. W.C. Chong, E. Mahmoudi, Y.T. Chung, M.M. B., C.H. Koo, A.W. Mohammad, Desalin Water Treat. Journal. **10**, 1-10 (2017)
21. M. Peydayesh, M. Bagheri, T. Mohammadi, O. Bakhtiari, RSC Adv. **7**, 24995-25008 (2017)
22. L. Huang, S. Zhao, Z. Wang, J. Wu, J. Wang, S. Wang, J Memb Sci. **499**, 269-281 (2016)
23. H. Song, F. Ran, H. Fan, X. Niu, L. Kang, C. Zhao, J Memb Sci. **471**, 319-327 (2014)
24. Z. Yang, Y. Wu, H. Guo, X.-H. Ma, C.-E. Lin, Y. Zhou, B. Cao, B.-K. Zhu, K. Shih, C.Y. Tang, J Memb Sci. **544**, 351-358 (2017)
25. M.S. Haider, G.N. Shao, S.M. Imran, S.S. Park, N. Abbas, M.S. Tahir, M. Hussain, W. Bae, H.T. Kim, Mater Sci Eng C Mater Biol Appl. **62**, 732-45 (2016)
26. R. Zhang, Y. Su, X. Zhao, Y. Li, J. Zhao, Z. Jiang, J Memb Sci. **470**, 9-17 (2014)
27. B. Vatsha, J.C. Ngila, R.M. Moutloali, Physics and Chemistry of the Earth, Parts A/B/C. **67-69**, 125-131 (2014)
28. D.Y. Koseoglu-Imer, B. Kose, M. Altinbas, I. Koyuncu, J Memb Sci. **428**, 620-628 (2013)